Atmos. Meas. Tech. Discuss., 5, 8969–8993, 2012
www.atmos-meas-tech-discuss.net/5/8969/2012/
doi:10.5194/amtd-5-8969-2012

Atmospheric Measurement Techniques Discussions

Selective measurements of NO, NO_2 and NO_y in the free troposphere using quantum cascade laser spectroscopy

B. Tuzson[1], K. Zeyer[1], M. Steinbacher[1], J. B. McManus[2], D. D. Nelson[2], M. S. Zahniser[2], and L. Emmenegger[1]

[1]Empa, Swiss Federal Laboratories for Materials Science and Technology, Laboratory for Air Pollution and Environmental Technology, Überlandstr. 129, 8600 Dübendorf, Switzerland
[2]Aerodyne Research, Inc., Center for Atmospheric and Environmental Chemistry, Billerica, MA 01821, USA

Received: 11 December 2012 – Accepted: 14 December 2012 – Published: 20 December 2012

Correspondence to: B. Tuzson (bela.tuzson@empa.ch)

Published by Copernicus Publications on behalf of the European Geosciences Union.

Abstract

A quantum cascade laser based absorption spectrometer for continuous and direct measurements of NO and NO_2 was employed at the high-altitude monitoring site Jungfraujoch (3580 m a.s.l., Switzerland) during a three month campaign in Spring/Summer 2012. The total reactive nitrogen, NO_y, was also measured in the form of NO after conversion on a gold catalyst. The aim was to assess the suitability of the instrument for long-term monitoring of the main reactive nitrogen species under predominantly free tropospheric air conditions. A precision (1σ) of 10 and 3 ppt for NO and NO_2 was achieved with 180 s averaging time under field conditions. The linear dynamic range of the instrument has been verified for both species from the detection limit to $\approx$ 45 ppbv. The spectrometer shared a common sampling inlet with a chemiluminescence-based analyzer. The comparison of the time series shows excellent agreement between the two techniques and demonstrates the adequacy of the laser spectroscopic approach for this kind of demanding environmental applications.

1 Introduction

In the troposphere, the abundance of reactive nitrogen species is primarily influenced by emissions from anthropogenic sources in the form of nitrogen oxides (NO_x = NO + NO_2). Once in the atmosphere, these species are involved in a number of different chemical pathways and oxidized to a large variety of other reactive nitrogen species denoted as NO_y (Crutzen, 1979; Logan, 1983). Despite their low atmospheric concentrations, nitrogen oxides represent an important factor regarding air quality given their contribution to local ozone production and secondary organic aerosol formation. Furthermore, the adverse effect of NO_2 on the human respiratory system and the formation of nitric acid (HNO_3), which is the dominant sink of NO_x (via dry and wet deposition), makes it a harmful air pollutant (Wesely and Hicks, 2000; Jacob, 2000). The significance of NO_x in tropospheric chemistry triggered the interest in instrumental

AMTD
5, 8969–8993, 2012

development. This is a challenging task given the substantial spatial and temporal variability of NO_x, which ranges from a few ppt at remote locations to > 100 ppb in urban regions. Nevertheless, it has been adressed over the last two decades by a wide variety of measurement techniques and by even larger number of instrumentation (see e.g. review by Clemitshaw (2004) and references therein). Although, recent intercomparison studies demonstrate that several techniques perform well (Fehsenfeld et al., 1990; Fuchs et al., 2010), they still involve research grade instruments that are not yet established as routine monitoring tools.

At present, chemiluminescence detection (CLD) is considered to be the standard technique and is commonly used in field missions and air quality monitoring (Demerjian, 2000; GAW Report #195, 2011). Although, the method has very good precision for NO, it is unable to directly measure NO_2. Nevertheless, this has successfully been overcome by including the conversion (catalytic or photolytic) of NO_2 to NO prior to analysis. Besides the necessity of systematic determination of the conversion efficiency, the conversion may also lead to interferences of other nitrogen compounds that can readily be converted to NO (Dunlea et al., 2007; Steinbacher et al., 2007), possibly resulting in overestimated NO_2 readings. The alternating measurement of NO and NO_x can also lead to artifacts in the NO_2 determination when the ambient NO_x levels experience rapid changes. Thus, a setup with two individual CLDs (three in case of NO, NO_x and NO_y observations) is the preferred – but not inexpensive – configuration.

For the present study, we adopted the dual laser design approach recently reported by McManus et al. (2010). Our choice for quantum cascade laser based direct absorption spectroscopy (QCLAS) was driven by two major factors: (i) our previous campaigns performed in a large variety of environments including grass-land, forest and mountain sites (Tuzson et al., 2008; Neftel et al., 2010; Kammer et al., 2011; Tuzson et al., 2011) showed that QCLAS is a robust and reliable technique to be employed under various field and measurement conditions and (ii) we obtained up to date the longest (more than four years of continuous operation) time-series of CO_2 isotope ratio measurements at a mountain site, which reflects the sturdy operation capability of the QCLs

AMTD
5, 8969–8993, 2012

(Sturm et al., 2013). In addition to these considerations, the direct absorption technique offers a simple and straightforward solution to perform absolute spectroscopic quantification of the molecular species of interest.

In the following sections we describe the laser instrument, the measurement strategy and the experimental setup used for the campaign to perform direct and simultaneous measurements of NO and NO_2. The validation of the time series recorded during three months of continuous operation is done against the standard CLD method. A short discussion is given on the discrepancy seen when employing the catalytic gold converter for NO_y measurements.

2 Experimental

2.1 Instrumentation

2.1.1 NO_x QCLAS

The spectroscopic instrument (Aerodyne Research, Inc., USA) employed in this study is based on continuous wave quantum cascade laser (cw-QCL) technology. A recent review on optical design, performance characteristics and application fields of this kind of analyzer has been presented by McManus et al. (2010). Briefly, the spectrometer embodies two room-temperature cw-QCLs (Alpes Lasers, Switzerland) emitting in the spectral range of 1600 and 1900 cm^{-1}, respectively. The individual laser beams are first collected by a pair of reflective objectives then combined and co-oriented by a dichroic mirror (LohnStar Optics, Inc., USA) and sent through a wedged beamsplitter that results in three different beams. The main beam is further shaped by a series of reflective optics and coupled into an astigmatic Herriott multipass absorption cell (AMAC-200) which folds the laser radiation for a total number of 434 reflections. This results in an effective path length of 204 m (McManus et al., 2011). When the exit condition of the cavity is fulfilled, the laser beam leaves the cell through the same entrance

AMTD
5, 8969–8993, 2012

hole and is then focused on a thermoelectrically cooled IR detector (Vigo Systems, Poland). The fraction of the laser beam reflected from the first surface of the beamsplitter is directed through a short (5 cm) cell filled with a 1 : 1 mixture of NO and NO_2 and subsequently aimed onto a second detector. This reference path assures the locking of the laser frequency to well defined absorption lines even in situations when the ambient NO_x concentrations drop below the limit of detection or when the multipass cell is filled with NO_x-scrubbed air for spectral background measurements. The third beam reflected from the back surface of the wedge is used for accurate frequency tuning rate determination of the lasers by placing a germanium etalon in its path. This beam is also focused onto the reference detector. A flipping mechanism selects between the two beams (reference cell or etalon).

Beside the optical assembly design, the electronics have also experienced some major improvements. A significant reduction of the hardware size has been achieved by moving towards USB-DAQ solution (NI USB-6251 OEM, National Instruments, Inc., USA) and embedded mini-PCs. Low noise laser drivers (Wavelength Electronics, Inc., USA) combined with dedicated power-supply design and thermal management led to unprecedented stability. Details regarding the laser control and spectral fitting software (TDLWintel, Aerodyne Research, Inc., USA) have been discussed previously (Nelson et al., 2004).

The major advantage of a direct spectroscopic detection of NO_2 is the immunity from interferences associated with photochemical conversion of NO_2 to NO prior to detection. However, this technique may suffer from interferences of other nature, such as overlapping absorption features from other molecular species or pressure broadening effects mainly due to water (Tuzson et al., 2010). Therefore, we performed a detailed investigation of the simulated absorption spectra, generated based on typical experimental parameters and the HITRAN database (Rothman et al., 2009), in the range of 1600 and 1900 cm^{-1}, where NO_2 and NO have their fundamental ro-vibrational modes. The aim was to select the strongest absorption lines possible with the stringent condition that the spectral interferences from water vapor or other trace gases are minimal.

AMTD
5, 8969–8993, 2012

The best compromises we could identify were the doublet lines located at 1900.0706 and 1900.0816 cm^{-1} for NO and the group of lines in the vicinity of 1599.9 cm^{-1} for NO_2 (see Fig. 1). Simulations of typical real-time scenarios involving low NO_x concentrations and various humidity levels indicated low interference effects (< 70 ppt NO_x per volume % H_2O), which was later confirmed experimentally. Based on these examinations, two cw-QCLs were selected correspondingly with single mode emission powers higher than 10 mW at the specified wavelengths.

The instrument's precision has been enhanced by addressing the issue of interference fringes. These are mainly produced by scattered light within the multipass cell and may significantly limit the achievable SNR improvement available from multipass cell's. They typically generate an absorption equivalent noise level of 10^{-4} in the background signal. A significant improvement was obtained by careful investigation and selection of circulation patterns that minimize fringes near the absorption line-width and by using high-reflectivity mirrors that lead to lower fringes by reducing the ratio of scattered light to transmitted light (McManus et al., 2011). In addition, a mechanical modulation (dithering) of the cell mirrors by a piezo-crystal helps to average out fringes. As a result, a precision of σ_{min} = 1 ppt for NO_2 after 12 min of averaging was achieved in the laboratory. Under field conditions, however, this performance may suffer from environmental influences. Therefore, the instrument's stability was investigated on-site by measuring NO_x-free air for a time period of one hour with a detection bandwidth of 1 Hz and calculating the associated Allan variance as a function of averaging time (Werle et al., 1993). This two-sample variance-plot is shown on Fig. 2 and allows to define the optimum calibration timescale. The variance curve reveals flicker noise contributions to the signal, manifested as deviations from the expected $1/\tau$ slope, at around 10 and 220 s. Similar behavior has been described by Werle (2011) and associated to optical fringes. Following his theoretical framework, it was possible to closely reproduce the observed deviations by assuming two periodic fringe components with frequencies of 4.3×10^{-2} Hz and 2.2×10^{-3} Hz, respectively. In fact, the 23 s periodicity correlates well with the PID-cycle of the temperature controller employed for stabilizing the optical

AMTD
5, 8969–8993, 2012

module. The slow fringe is probably due to opto-mechanical drifts or variations in the driver electronics, reflecting the temperature fluctuations (≈ 4 K) experienced at the monitoring station. Taking into account this behavior, we lowered the averaging time by about a factor four compared to the laboratory situation. Nevertheless, the precision achieved at the monitoring site after 180 s averaging time was 3 and 10 ppt, which corresponds to an absorbance noise level of 5.9×10^{-6} and 8.8×10^{-6} for NO_2 and NO, respectively. Normalizing to the 204 m optical path-length, this corresponds to an absorbance per unit path length sensitivity of 5×10^{-10} cm^{-1}.

The strategy to cope with this flicker noise issue was the frequent and periodic background (zero-air) spectrum subtraction from the measured spectrum. Therefore, a cost effective NO_x filter that consists of a stainless-steel container (1 L) filled with grained activated charcoal (Merck KGaA, Germany) was used to generate NO_x-scrubbed air for spectral background measurements. The NO_x filter efficiency has been verified in comparison with high purity (5.5) He and N_2. The filter solution was the preferred method over the use of dry N_2 as zero-air, because the NO_x filter does not significantly alter the water vapor mixing ratio of the air flowing through it, and thus, the zero-air better reconciles the sampled air humidity and contributes in reducing possible detection artifacts that could be induced by spectral interferences due to water absorption lines. The most efficient method to maintain the best stability and accuracy of the spectrometer has been achieved by automatically recording a background spectrum every 10 min and subtracting it from each subsequent sample spectrum before fitting. More details about the measurement cycle are presented in the Section 3.

2.1.2 Chemiluminescence NO_x detection

The routine, long-term monitoring of NO, NO_x and NO_y at the Jungfraujoch is performed with commercially available chemiluminescence analyzers (CraNOx, Eco Physics, Switzerland). The chemiluminescence detection (CLD) technique, developed in the 1970s, is the reference method recommended by the US EPA (Demerjian, 2000) and by European legislation (European Standard, EN 14211, 2012) for the

AMTD
5, 8969–8993, 2012

measurement of NO_x in monitoring networks. The method relies on the light emission from the electronically excited NO_2, a product generated in the gas-phase reaction of ambient NO with O_3 added in excess to the air sample. The emission intensity is directly proportional to the concentration of NO in the air, and the emitted photons are detected by a photo multiplier tube. NO_x is measured as NO after photolytic conversion of NO_2. The atmospheric NO_2 is then derived by subtraction of NO from the NO_x signal (Ridley and Howlett, 1974; Ryerson et al., 2000; Sadanaga et al., 2010). NO_y species are converted to NO on a heated gold catalyst (300 °C) in the presence of CO as a reducing agent (Fahey et al., 1985).

The measurement procedure as well as the calibration strategy has repeatedly been described in detail (Zellweger et al., 2000; Pandey Deolal et al., 2012). Here we just recall that for the sensitive measurement of the NO-NO_x-NO_y species, three dedicated CLDs are used. The detection limits of the CLDs for NO and NO_y after 2 min averaging are 20 ppt, whereas it is 50 ppt for the NO_2 channel due to the incomplete conversion and the determination of NO_2 by the difference of two measured (NO and NO + converted NO_2) signals. The overall measurement uncertainty (1 σ) is 9 % for NO_y and 5 % for NO_x, including CLD precision, the NO standard uncertainty, and the conversion efficiencies of the photolytic convertor (PLC). Data are processed and reported as 10 min averages.

Since the PLC-CLD setup is used as the standard method, these measurements are taken as reference for validating the QCLAS data.

2.2 Site description and sampling setup

Field measurements took place between 22 March and 25 June 2012 at the high alpine research station Jungfraujoch (JFJ, 46.55 °N, 7.98 °E , elevation 3580 m). The monitoring station is one of the 28 global sites of the Global Atmosphere Watch (GAW) program of the World Meteorological Organization (WMO). Given its location, the air sampled here is expected to be representative for the lower free troposphere over Europe, which is mainly the case in the autumn and winter season, while in late spring and summer it

AMTD
5, 8969–8993, 2012

can be influenced by the planetary boundary layer (Baltensperger et al., 1997; Lugauer et al., 1998; Zellweger et al., 2003). Long term continuous in-situ monitoring of trace gases such as NO, NO_2, NO_y, CO, and O_3 is routinely performed by Empa within the activities of the Swiss National Air Pollution Monitoring Network (NABEL).

The ambient air was sampled using the main inlet of the monitoring site. It consists of a heated stainless steel inlet (inner diameter 9 cm) situated about 3 m above ground, in which the ambient air is drawn at a high flow rate of $> 800\,L\,min^{-1}$ (Fig. 3). The main manifold is temperature controlled to keep the gas temperature at its lower end at constant 10 °C. Potential losses of NO_y in the sampling lines are minimized by placing the gold converter close to the main inlet, connected with about 1 m long PFA tubing. The time required for the air to reach the converter is about 2 s. The photolytic converter (PLC 762, Eco Physics, Switzerland) for the NO_2 measurement is placed next to the NO_y converter. Downstream of the converters, the air is drawn through separate PFA tubing to the chemiluminescence analyzers. The air for the NO analysis is drawn directly from the main manifold with PFA tubing.

The NO analyzers are automatically calibrated every 39 h by measuring zero air and NO standard gas (5 ppm NO in N_2, referenced against NIST Standard Reference Material (SRM 2629a) and NMI Primary Reference Material (PRM BD11)) diluted with zero air to approximately 48 ppb. The conversion efficiency of the converter is determined by gas phase titration of NO with ozone every 78 h. The conversion efficiency of the PLC usually ranged from 74 to 58 %.

The QCLAS was operated alongside the CLDs for the duration of the study. An additional gold converter (CON 765, Eco Physics, Switzerland) was mounted next to the NABEL NO_y converter and shared the same CO source (purity 99.997 %, Messer-Griesheim GmbH), whereas the sampling line was independently connected to the main inlet. The selection between ambient air and air passing through the gold converter was accomplished by a 3-way all-Teflon solenoid valve (Teqcom Ind., USA). The flow rate of $1\,L\,min^{-1}$ was manually adjusted by a PTFE needle valve V_M (PKM, Switzerland) mounted upstream of the cell (see Fig. 3), while the cell pressure

AMTD
5, 8969–8993, 2012

(≃ 50 hPa) was established by selecting the appropriate pumping rate with an integrated potentiometer on the oil-free diaphragm pump (N920 series, KNF, Germany). Measurements were taken continuously at 1 s time resolution and post-processed to meet the 10 min averaging time scale of the CLD.

3 Results and discussion

For free tropospheric air composition monitoring, high instrumental precision alone is not sufficient to obtain the necessary accuracy. In fact, an optimal calibration and sampling strategy is equally important and has a decisive influence on the data quality. The strategy employed in this study exploits the very high precision and the fast response of the instrument when measuring zero-air. It consists of various steps repeated in half-hour sequence. First, a background spectrum is recorded using NO_x-scrubbed air as described in the previous section. This is achieved by directing the sampled ambient air through the NO_x filter by switching the solenoid valve V_3 (see Fig. 3) and purging the absorption cell for 120 s. The last 10 s are then averaged and used to determine the spectral baseline and perform a background correction by subtracting it from all the subsequent spectra. The second step involves measuring NO and NO_2 simultaneously by drawing sample air directly through the absorption cell. In the next step, the solenoid valve V_1 is switched together with V_2 to divert the air flow across the gold converter and thus, the NO_y mixing ratio is measured as NO. The NO_2 signal can later be used to verify the converter efficiency for NO_2 or to monitor baseline changes due to humidity variations or potential instrumental drifts. After a 10 min measurement period, the system is switched back to direct ambient air sampling. Finally, zero-air is measured again as another background spectrum, which is used in a post-processing step for drift correction. For more confidence in the "absolute" zero baseline determination, dry N_2 from a gas cylinder (purity 5.5) is measured instead of NO_x-scrubbed air every second hour. This acts as an additional parameter for monitoring the performance of the NO_x filter and also aids in establishing the water vapor induced interferences, which can be

AMTD
5, 8969–8993, 2012

applied to correct the measurement values. The amount of this correction was empirically determined as being −16.8 ± 3.7 ppt NO and −57.3 ± 3.5 ppt NO_2 for 1 % volume H_2O. The air humidity at JFJ was measured by the QCLAS simultaneously with the NO_x and it was below 0.3 % during the whole campaign. Thus, the water vapor effect was rather marginal leading to a minor correction only, i.e. 5 to 20 ppt at most, in the measured NO and NO_2 values.

Dynamic dilutions of standard NO_2 and NO gases were used to establish the span of the laser spectrometer for the NO_x measurements from the detection limit up to 50 ppbv, and to calibrate the purely spectroscopic data against the standard-scale used by NABEL (see Fig. 4 and previous Section). The accuracy of this calibration is dominated by the accuracy of the mass flow controllers (MFCs) used for the dilution. These MFCs (Red-y smart series, Voegtlin, Switzerland) were referenced against a high-accuracy venturi flow-meter (molbloc, DH Instruments/Fluke, USA) at Empa. Since NO_2 gas mixtures in cylinders are known to be unstable, the NO_2 concentration (96.3 ± 3.7 ppb) was first determined with a calibrated CLD followed by QCLAS measurements and dynamic dilution (Fig. 4). The sampling line was taken the same and thus, we assumed that losses of NO_2 on the metallic surfaces of the pressure regulator and MFCs are similar. Obviously, the total uncertainty in this case is mainly given by systematic errors due to losses.

It is noted that all above mentioned parameters were determined on site, i.e. at the monitoring station JFJ. This assured a direct link to the retrieved tropospheric NO_x data. Figure 5 shows an exemplary window of 21 days from the time series recorded by both techniques during the three months campaign. The challenge of such tropospheric air measurements is well illustrated by the NO data, where ∼ 78 % of the values are below 0.1 ppb. Despite of this, the variations in the mixing ratio profiles of NO and NO_2 compare very well between the CLD and the QCLAS. The quantitative agreement is illustrated on Fig. 6 in the form of correlation plots for NO_x and NO_y measured during the three months campaign. The unity slopes with zero intercept are also shown as reference. The calibrated QCLAS data were averaged to 10 min time resolution to

AMTD
5, 8969–8993, 2012

match the CraNOx time scale. In order to minimize the scatter due to synchronization differences between instruments, the error of the mean of each individual value was taken as a measure of the variance during that time window and was used to filter out data points which exhibited too large short-term variations. Statistical analysis on the differences between all NO_x data reported by the two analyzers showed that more than 94 % of individual data points agree to within ± 50 ppt, which is in the same order as the detection limit of the CLD.

In the case of the NO_y time-series, we observed a systematic discrepancy of about 0.26 ppb, which, over the measurement period, displayed short-term (< 12 h) variations of up to 1.2 ppb. Additional tests, involving different gases (ambient air, dry N_2 and diluted NO standard) as common input sample to the converters and alternating measurements with QCLAS and CLD, revealed that the two converters generate indeed different amounts of NO_y in excellent agreement with the discrepancy seen for the time-series. Figure 7 shows the clear bias seen by the QCLAS when switching between the two Au converters sharing the same inlet with diluted NO standard as sample gas. The difference disappeared only when dry N_2 was flowing through the converters. Therefore, the mismatch between the two gold-converters has been attributed to their slightly different conversion efficiencies. Even though, for NO_2, the converters' efficiencies were found comparable (within 1.5 %), Au catalyst may have different efficiencies for the various reactive nitrogen species or may suffer from contributions of other interfering compounds. According to systematic investigations, species such as nitric acid (HNO_3) and peroxyacyl nitrates (PANs) have conversion efficiencies higher than 95 %, whereas ammonia (NH_3) and hydrogen cyanide (HCN) in the presence of water vapor show little but variable contribution (1–5 %), and their magnitude depends on the surface history and temperature of the converter (Kliner et al., 1997; Fahey et al., 1985; Volz-Thomas et al., 2005). Although, we had no speciation measurements for these compounds, literature data allow for an estimate of their contribution. Partitioning measurements of NO_y in the lower free troposphere (Zellweger et al., 2003) revealed that PAN is the dominant NO_y species (∼ 38 %) during spring, whereas HNO_3 has a minor

AMTD
5, 8969–8993, 2012

contribution (< 20 ppt). Mixing ratio values of ∼ 200 ppt for HCN at the JFJ were reported by Rinsland et al. (2000). Using the above values, a difference of about 14 % in the conversion efficiencies for PAN is necessary to explain the observed mismatch between the converters. Such a large difference in the converter's efficiency is surprising at first sight. However, we also observed a significant difference in the CO_2 content of the gas samples after the converters despite the similar CO flow rates (see Fig. 3). While the CO_2 level remained unchanged after passing through the converter with lower NO_y values, the other converter almost doubled the amount of CO_2.

Finally, it should be noted that slightly lower NO_y values (6–10 %) in the NABEL system have already been observed during intercomparison campaigns (Zellweger et al., 2003; Pandey Deolal et al., 2012), but they were attributed to potential losses of HNO_3 in the inlet system. This, however, has to be reconsidered and further investigations of Au converter's inter-comparability is recommended.

4 Conclusions

The validation and long-term performance assessment of a quantum cascade laser spectrometer was successfully accomplished at the high altitude research station JFJ by measuring the tropospheric NO_x and NO_y mixing ratios accompanied by standard monitoring CLD technique. To our knowledge, this is the first intercomparison study of this kind, involving a laser absorption technique for direct and simultaneous measurement of both, NO and NO_2, under field conditions. The time-series recorded by QCLAS show very good correlation with the CLD data even at sub-ppb mixing ratio levels. A dedicated gas sampling/handling method combined with the high instrumental precision (< 10 ppt) delivered the accuracy and drift suppression needed for reliable background tropospheric air NO_x monitoring. Since both techniques give similar results, there is no fundamental reason to replace the well established and reliable CLD technique by QCLAS. Nevertheless, the possibility to detect NO_2 selectively, i.e. without chemical conversion, and with high time resolution (1 Hz) is very attractive.

AMTD
5, 8969–8993, 2012

Furthermore, significant advances in quantum cascade laser technology lets us anticipate the appearance of compact multi-color sources, which would lead to substantial simplification of the optical design resulting in more robust, compact, and cost-effective analyzers.

The intercomparison of the NO_y data revealed differences which could not be attributed to any of the measurement techniques, but rather has been associated with the conversion efficiency of the gold catalyst. This was confirmed in a dedicated set of experiments, but the exact reason for the different behavior of the two seemingly identical catalysts remains unclear.

Acknowledgements. This work was supported by the Federal Office for the Environment (FOEN), Switzerland and the Swiss National Science Foundation (SNSF/R'Equip). We thank the International Foundation High Altitude Research Stations Jungfraujoch and Gornergrat (HFSJG) for access to the facilities at the Research Station Jungfraujoch and the custodians for on-site support. Beat Schwarzenbach (Empa) is acknowledged for calibrating our NO_2 working standard. We also acknowledge the valuable contributions of Ryan McGovern, Stanley Huang and Michael Agnese (ARI).

References

Baltensperger, U., Gäggeler, H. W., Jost, D. T., Lugauer, M., Schwikowski, M., Weingartner, E., and Seibert, P.: Aerosol climatology at the high-alpine site Jungfraujoch, Switzerland, J. Geophys. Res-Atmos., 102, 19707–19715, doi:10.1029/97JD00928, 1997. 8977

Clemitshaw, K. C.: A review of instrumentation and measurement techniques for ground-based and airborne field studies of gas-phase tropospheric chemistry, Crit. Rev. Env. Sci. Tec., 34, 1–108, doi:10.1080/10643380490265117, 2004. 8971

Crutzen, P. J.: The role of NO and NO_2 in the chemistry of the troposphere and stratosphere, Annu. Rev. Earth Pl. Sc., 7, 443–472, doi:10.1146/annurev.ea.07.050179.002303, 1979. 8970

Demerjian, K. L.: A review of national monitoring networks in North America, Atmos. Environ., 34, 1861–1884, doi:10.1016/S1352-2310(99)00452-5, 2000. 8971, 8975

AMTD

5, 8969–8993, 2012

Dunlea, E. J., Herndon, S. C., Nelson, D. D., Volkamer, R. M., San Martini, F., Sheehy, P. M., Zahniser, M. S., Shorter, J. H., Wormhoudt, J. C., Lamb, B. K., Allwine, E. J., Gaffney, J. S., Marley, N. A., Grutter, M., Marquez, C., Blanco, S., Cardenas, B., Retama, A., Ramos Villegas, C. R., Kolb, C. E., Molina, L. T., and Molina, M. J.: Evaluation of nitrogen dioxide chemiluminescence monitors in a polluted urban environment, Atmos. Chem. Phys., 7, 2691–2704, doi:10.5194/acp-7-2691-2007, 2007. 8971

Fahey, D. W., Eubank, C. S., Hubler, G., and Fehsenfeld, F. C.: Evaluation of a catalytic reduction technique for the measurement of total reactive odd-nitrogen NO_y in the atmosphere, J. Atmos. Chem., 3, 435–468, doi:10.1007/BF00053871, 1985. 8976, 8980

Fehsenfeld, F. C., Williams, E. J., Buhr, M. P., Hübler, G., Langford, A. O., Murphy, P. C., Parrish, D. D., Norton, R. B., Fahey, D. W., Drummond, J. W., Mackay, G. I., Roychowdhury, U. K., Hovermale, C., Mohnen, V. A., Demerjian, K. L., Galvin, P. J., Calvert, J. G., Ridley, B. A., Grahek, F., Heikes, B. G., Kok, G. L., Shetter, J. D., Walega, J. G., Elsworth, C. M., and Schiff, H. I.: Intercomparison of NO_2 measurement techniques, J. Geophys. Res., 95, 3579–3597, doi:10.1029/JD095iD04p03579, 1990. 8971

Fuchs, H., Dubé, W. P., Lerner, B. M., Wagner, N. L., Williams, E. J., and Brown, S. S.: A sensitive and versatile detector for atmospheric NO_2 and NO_x based on blue diode laser cavity ring-down spectroscopy, Environ. Sci. Technol., 43, 7831–7836, doi:10.1021/es902067h, 2009.

Fuchs, H., Ball, S. M., Bohn, B., Brauers, T., Cohen, R. C., Dorn, H.-P., Dubé, W. P., Fry, J. L., Häseler, R., Heitmann, U., Jones, R. L., Kleffmann, J., Mentel, T. F., Müsgen, P., Rohrer, F., Rollins, A. W., Ruth, A. A., Kiendler-Scharr, A., Schlosser, E., Shillings, A. J. L., Tillmann, R., Varma, R. M., Venables, D. S., Villena Tapia, G., Wahner, A., Wegener, R., Wooldridge, P. J., and Brown, S. S.: Intercomparison of measurements of NO_2 concentrations in the atmosphere simulation chamber SAPHIR during the NO3Comp campaign, Atmos. Meas. Tech., 3, 21–37, doi:10.5194/amt-3-21-2010, 2010. 8971

GAW Report #195. A WMO/GAW Expert Workshop on Global Long-term Measurements of Nitrogen Oxides and Recommendations for GAW Nitrogen Oxides Network (WMO TD No. 1570), available at: www.wmo.int/pages/prog/arep/gaw/documents/Final_GAW_195_TD_No_1570_web.pdf, 2011. 8971

Jacob, D. J.: Heterogeneous chemistry and tropospheric ozone, Atmos. Environ., 34, 2131–2159, doi:10.1016/S1352-2310(99)00462-8, 2000. 8970

AMTD
5, 8969–8993, 2012

Kammer, A., Tuzson, B., Emmenegger, L., Knohl, A., Mohn, J., and Hagedorn, F.: Application of a quantum cascade laser-based spectrometer in a closed chamber system for real-time $\delta^{13}C$ and $\delta^{18}O$ measurements of soil-respired CO_2, Agr. Forest Meteorol., 151, 39–48, doi:10.1016/j.agrformet.2010.09.001, 2011. 8971

Kley, D., Drummond, J. W., McFarland, M., and Liu, S. C.: Tropospheric profiles of NO_x, J. Geophys. Res., 86, 3153–3161, doi:10.1029/JC086iC04p03153, 1981.

Kliner, D. A. V., Daube, B. C., Burley, J. D., and Wofsy, S. C.: Laboratory investigation of the catalytic reduction technique for measurement of atmospheric NO_y, J. Geophys. Res.-Atmos., 102, 10759–10776, doi:10.1029/96JD03816, 1997. 8980

Logan, J. A.: Nitrogen oxides in the troposphere: global and regional budgets, J. Geophys. Res., 88, 10785–10807, doi:10.1029/JC088iC15p10785, 1983. 8970

Lugauer, M., Baltensperger, U., Furger, M., Gäggeler, H. W., Jost, D. T., Schwikowski, M., and Wanner, H.: Aerosol transport to the high Alpine sites Jungfraujoch (3454 m a.s.l.) and Colle Gnifetti (4452 m a.s.l.), Tellus B, 50, 76–92, doi:10.1034/j.1600-0889.1998.00006.x, 1998. 8977

McManus, J. B., Zahniser, M. S., Nelson, D. D., Shorter, J. H., Herndon, S., Wood, E., and Wehr, R.: Application of quantum cascade lasers to high-precision atmospheric trace gas measurements, Opt. Eng., 49, 111124–111135, doi:10.1117/1.3498782, 2010. 8971, 8972

McManus, J. B., Zahniser, M. S., and Nelson, D. D.: Dual quantum cascade laser trace gas instrument with astigmatic Herriott cell at high pass number, Appl. Opt., 50, A74–A85, doi:10.1364/AO.50.000A74, 2011. 8972, 8974

Neftel, A., Ammann, C., Fischer, C., Spirig, C., Conen, F., Emmenegger, L., Tuzson, B., and Wahlen, S.: N_2O exchange over managed grassland: Application of a quantum cascade laser spectrometer for micrometeorological flux measurements, Agr. Forest Meteorol., 150, 775–785, doi:10.1016/j.agrformet.2009.07.013, 2010. 8971

Nelson, D. D., McManus, B., Urbanski, S., Herndon, S., and Zahniser, M. S.: High precision measurements of atmospheric nitrous oxide and methane using thermoelectrically cooled mid-infrared quantum cascade lasers and detectors, Spectrochim. Acta A, 60, 3325–3335, doi:10.1016/j.saa.2004.01.033, 2004. 8973

Pandey Deolal, S., Brunner, D., Steinbacher, M., Weers, U., and Staehelin, J.: Long-term in situ measurements of NO_x and NO_y at Jungfraujoch 1998–2009: time series analysis and evaluation, Atmos. Chem. Phys., 12, 2551–2566, doi:10.5194/acp-12-2551-2012, 2012. 8976, 8981

AMTD
5, 8969–8993, 2012

Ridley, B. A. and Howlett, L. C.: An instrument for nitric oxide measurements in the stratosphere, Rev. Sci. Instrum., 45, 742–748, doi:10.1063/1.1686726, 1974. 8976

Rinsland, C. P., Mahieu, E., Zander, R., Demoulin, P., Forrer, J., and Buchmann, B.: Free tropospheric CO, C_2H_6, and HCN above central Europe: Recent measurements from the Jungfraujoch station including the detection of elevated columns during 1998, J. Geophys. Res-Atmos., 105, 24235–24249, doi:10.1029/2000JD900371, 2000. 8981

Rothman, L. S., Gordon, I. E., Barbe, A., Chris Benner, D., Bernath, P. F., Birk, M., Boudon, V., Brown, L. R., Campargue, A., Champion, J.-P., Chance, K., Coudert, L. H., Dana, V., Devi, V. M., Fally, S., Flaud, J. -M., Gamache, R. R., Goldman, A., Jacquemart, D., Kleiner, I., Lacome, N., Lafferty, W. J., Mandin, J.-Y., Massie, S. T., Mikhailenko, S. N., Miller, C. E., Moazzen-Ahmadi, N., Naumenko, O. V., Nikitin, A. V., Orphal, J., Perevalov, V. I., Perrin, A., Predoi-Cross, A., Rinsland, C. P., Rotger, M., Šimečková, M., Smith, M. A. H., Sung, K., Tashkun, S. A., Tennyson, J., Toth, R. A., Vandaele, A. C., and Vander Auwera, J.: The HITRAN 2008 molecular spectroscopic database, J. Quant. Spectrosc. Ra., 110, 533–572, doi:10.1016/j.jqsrt.2009.02.013, 2009. 8973

Ryerson, T. B., Williams, E. J., and Fehsenfeld, F. C.: An efficient photolysis system for fast-response NO_2 measurements, J. Geophys. Res-Atmos., 105, 26447–26461, doi:10.1029/2000JD900389, 2000. 8976

Sadanaga, Y., Fukumori, Y., Kobashi, T., Nagata, M., Takenaka, N., and Bandow, H.: Development of a selective light-emitting diode photolytic NO_2 converter for continuously measuring NO_2 in the atmosphere, Anal. Chem., 82, 9234–9239, doi:10.1021/ac101703z, 2010. 8976

Steinbacher, M., Zellweger, C., Schwarzenbach, B., Bugmann, S., Buchmann, B., Ordóñez, C., Prevot, A. S. H., and Hueglin, C.: Nitrogen oxide measurements at rural sites in Switzerland: bias of conventional measurement techniques, J. Geophys. Res-Atmos., 112, D11307, doi:10.1029/2006JD007971, 2007. 8971

Sturm, P., Tuzson, B., Henne, S., and Emmenegger, L.: Tracking isotopic signatures of CO_2 at Jungfraujoch with laser spectroscopy: analytical improvements and exemplary results, Atmos. Meas. Tech., in preparation, 2013. 8972

Tuzson, B., Mohn, J., Zeeman, M. J., Werner, R. A., Eugster, W., Zahniser, M. S., Nelson, D. D., McManus, J. B., and Emmenegger, L.: High precision and continuous field measurements of $\delta^{13}C$ and $\delta^{18}O$ in carbon dioxide with a cryogen-free QCLAS, Appl. Phys. B, 92, 451–458, doi:10.1007/s00340-008-3085-4, 2008. 8971

AMTD
5, 8969–8993, 2012

Tuzson, B., Hiller, R. V., Zeyer, K., Eugster, W., Neftel, A., Ammann, C., and Emmenegger, L.: Field intercomparison of two optical analyzers for CH_4 eddy covariance flux measurements, Atmos. Meas. Tech., 3, 1519–1531, doi:10.5194/amt-3-1519-2010, 2010. 8973

Tuzson, B., Henne, S., Brunner, D., Steinbacher, M., Mohn, J., Buchmann, B., and Emmenegger, L.: Continuous isotopic composition measurements of tropospheric CO_2 at Jungfraujoch (3580 m a.s.l.), Switzerland: real-time observation of regional pollution events, Atmos. Chem. Phys., 11, 1685–1696, doi:10.5194/acp-11-1685-2011, 2011. 8971

Volz-Thomas, A., Berg, M., Heil, T., Houben, N., Lerner, A., Petrick, W., Raak, D., and Pätz, H.-W.: Measurements of total odd nitrogen (NO_y) aboard MOZAIC in-service aircraft: instrument design, operation and performance, Atmos. Chem. Phys., 5, 583–595, doi:10.5194/acp-5-583-2005, 2005. 8980

Werle, P.: Accuracy and precision of laser spectrometers for trace gas sensing in the presence of optical fringes and atmospheric turbulence, Appl. Phys. B, 102, 313–329, doi:10.1007/s00340-010-4165-9, 2011. 8974

Werle, P., Mücke, R., and Slemr, F.: The limits of signal averaging in atmospheric trace-gas monitoring by tunable diode-laser absorption spectroscopy (TDLAS), Appl. Phys. B, 57, 131–139, doi:10.1007/BF00425997, 1993. 8974

Wesely, M. L. and Hicks, B. B.: A review of the current status of knowledge on dry deposition, Atmos. Environ., 34, 2261–2282, doi:10.1016/S1352-2310(99)00467-7, 2000. 8970

Zellweger, C., Ammann, M., Buchmann, B., Hofer, P., Lugauer, M., Rüttimann, R., Streit, N., Weingartner, E., and Baltensperger, U.: Summertime NO_y speciation at the Jungfraujoch, 3580 m above sea level, Switzerland, J. Geophys. Res-Atmos., 105, 6655–6667, doi:10.1029/1999JD901126, 2000. 8976

Zellweger, C., Forrer, J., Hofer, P., Nyeki, S., Schwarzenbach, B., Weingartner, E., Ammann, M., and Baltensperger, U.: Partitioning of reactive nitrogen (NO_y) and dependence on meteorological conditions in the lower free troposphere, Atmos. Chem. Phys., 3, 779–796, doi:10.5194/acp-3-779-2003, 2003. 8977, 8980, 8981

AMTD
5, 8969–8993, 2012

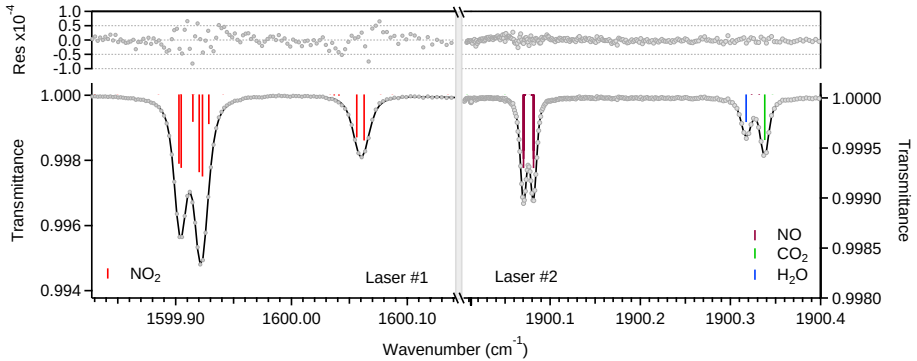

Fig. 1. The selected spectral windows with the absorption lines of NO and NO_2 as measured in ambient air with the dual-laser spectrometer with a multi-pass cell of 204 m path-length at 50 hPa sample pressure. The gray circles indicate measurement points, while the black line is a least-square fit to the data. The residual is shown in the top panel. The colored sticks indicate individual absorption lines of molecules that absorb within the scanning range of the lasers.

AMTD
5, 8969–8993, 2012

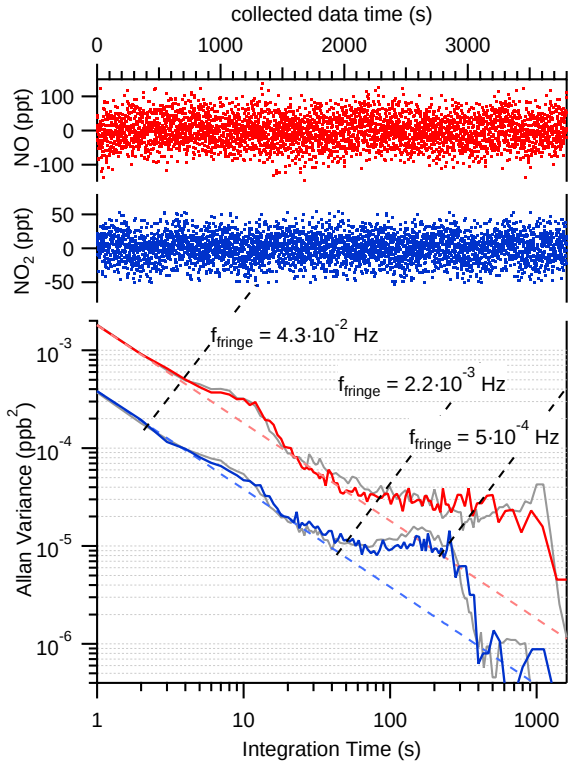

Fig. 2. Allan variance plots for NO and NO_2 measured with the dual-laser instrument at the Jungfraujoch using NO_x-free air as gas sample. The gray lines correspond to calculated white noise plus fringes contributing as flicker noise (details in text).

AMTD
5, 8969–8993, 2012

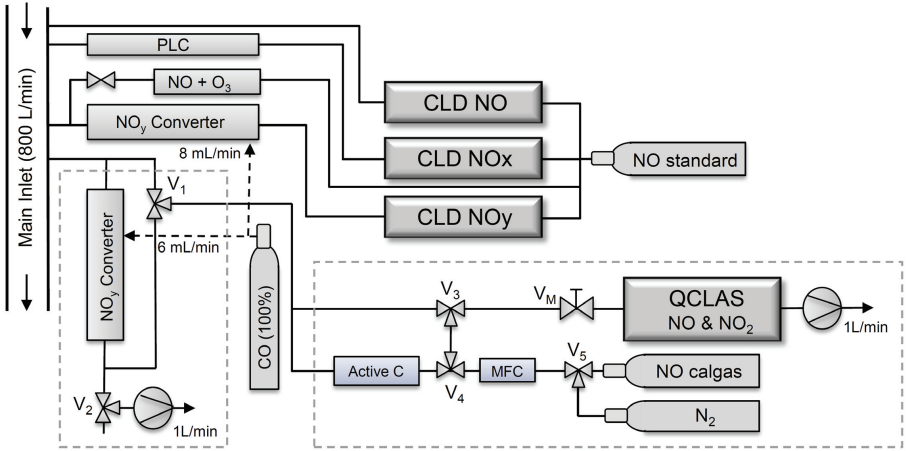

Fig. 3. Experimental setup at Jungfraujoch. The equipment within the dashed boxes was operated for a three month period, while the other instrumentation is part of the permanent monitoring program.

AMTD
5, 8969–8993, 2012

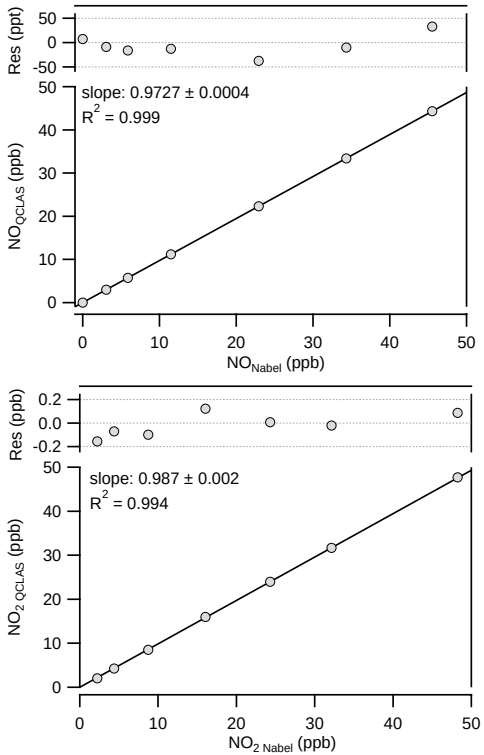

Fig. 4. Calibration plots of the QCLAS data for NO and NO_2. The abscissa represents the values determined from standard gas dilution (details in text), the fit (black line) is determined by weighted orthogonal distance regression and its residual is shown in the upper part.

AMTD
5, 8969–8993, 2012

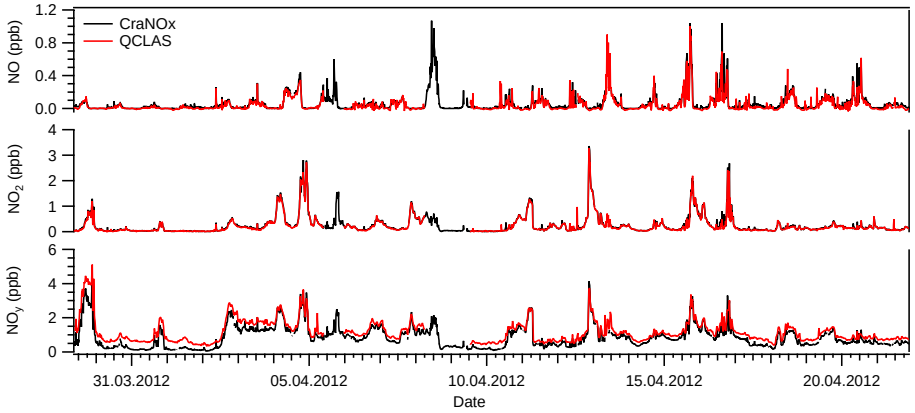

Fig. 5. An exemplary sequence of NO, NO_2 and NO_y time series measured at the Jungfraujoch with the two different methods. Note the different scaling of the y-axis. The gaps in the QCLAS data were caused by additional on-site works, such as calibration and converter investigation (see details in text).

AMTD
5, 8969–8993, 2012

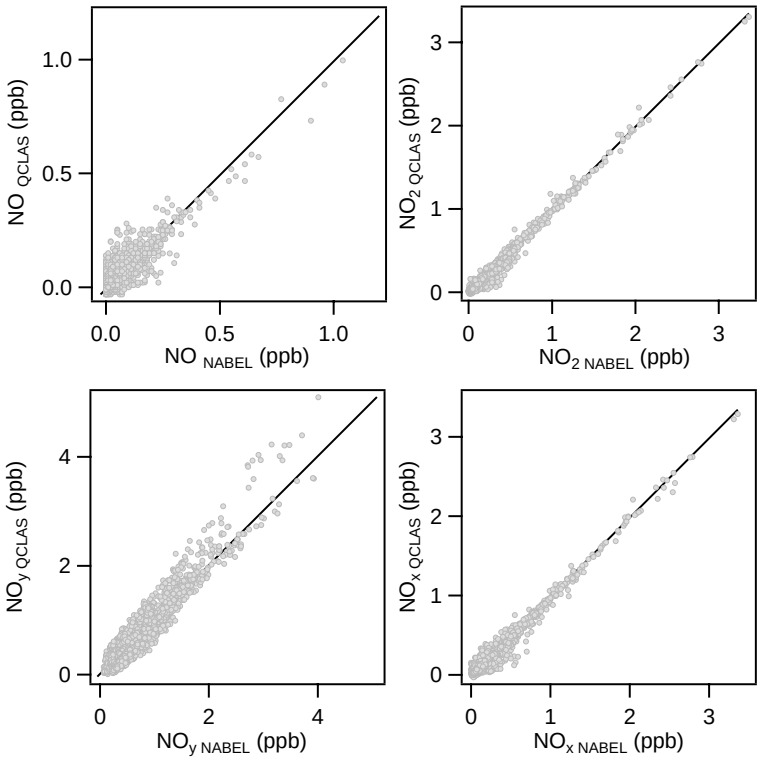

Fig. 6. Correlation plots of the QCLAS and CraNOx data. The 1 : 1 correlation is represented by the black line.

AMTD
5, 8969–8993, 2012

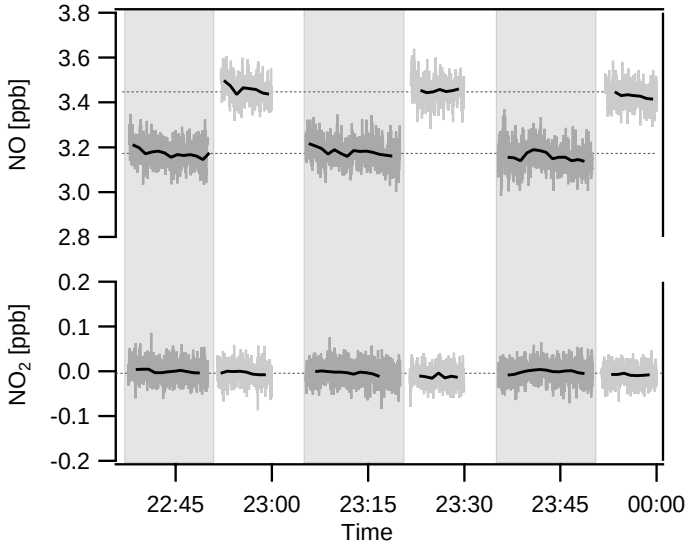

Fig. 7. NO and NO_2 mixing ratios measured with the QCLAS when switching between the two gold converters measuring NO standard gas diluted with "zero"-air. The gray areas correspond to the measurements of the converter used by the NABEL monitoring instrumentation.

AMTD
5, 8969–8993, 2012